journal

J. Am. Ceram. Soc., **80** [5] 1256–62 (1997)

Pressureless Sintering of Si_3N_4 Ceramic Using AlN and Rare-Earth Oxides

Zhen-Kun Huang, Anatoly Rosenflanz,* and I-Wei Chen*

Materials Science and Engineering, University of Michigan, Ann Arbor, Michigan 48109–2136

Using intermediate, liquid-forming compositions in the $(Y,La)_2O_3$–AlN system as additives, fully dense Si_3N_4 ceramics with high strength at high temperature have been obtained by pressureless sintering. The ceramics contain rod-shaped β-Si_3N_4 with M′ or K′ solid solutions as grain-boundary phases. The strength of these ceramics is 1150 MPa at 1200°C, and the room-temperature toughness is maintained at } 7 MPa·m$^{1/2}$. Phase relations that are pertinent to the new additive compositions are delineated to rationalize their beneficial effects on sinterability and mechanical properties.

I. Introduction

SINTERING of Si_3N_4 ceramics generally relies upon the liquid that forms from the native oxide layer of Si_3N_4 powders and the oxide sintering additives. The resultant ceramics can achieve high strength and high toughness at room temperature, provided a high density is reached and a network of elongated β-Si_3N_4 (or its solid solution, i.e., β-SiAlON) is developed.[1–3] For a given sintering condition, e.g., temperature, atmosphere, and time, the liquid composition has a direct influence on the kinetics of densification and grain shape development. Low-melting liquid is desirable in this regard. On the other hand, because a residual glassy phase always remains in the grain boundaries in Si_3N_4 ceramics after sintering, a loss of strength is experienced at temperatures above the glass softening point. Identification of sintering aids that simultaneously lead to superior sinterability, a well-developed β-Si_3N_4 network, and a refractory grain-boundary phase of a minimum amount has proved to be challenging.

An early approach to the above problem utilizes transient liquid-phase sintering. For example, by adding Al_2O_3 and AlN to Si_3N_4, it is possible to form a liquid in the transient stage during sintering, with the overall composition lying along the β-SiAlON line, $Si_{6-x}Al_xO_xN_{8-x}$.[4] Although the phase diagram indicates that no liquid should remain after sintering is complete and equilibrium is reached, in practice a grain-boundary glass remains in this system. Moreover, because β-SiAlON is structurally weaker and softer than β-Si_3N_4, the resultant ceramic has inferior mechanical properties. Generally, the incorporation of Al_2O_3 as a sintering aid has been found to be deleterious to high-temperature strength.[5,6] This presumably is because of the relatively low eutectic temperature of SiO_2 and Al_2O_3, in combination with many other oxides.[7]

In recent years, two alternative approaches have been developed to incorporate sintering aids into silicon nitrides with the purpose of improved high-temperature strength. The first approach focuses on the Si_3N_4–R_2O_3 binary, where R_2O_3 is any rare-earth oxide (or Y_2O_3) used singly or severally.[8–11] After sintering, this composition forms β-Si_3N_4 and some refractory rare-earth silicon oxynitrides (e.g., melilite (M-phase) $R_2Si_3O_3N_4$, wollastonite (K-phase) $RSiO_2N$, apatite (H-phase $R_5(SiO_4)_3N$, or rare-earth silicates, e.g., $R_2Si_2O_7$ and R_2SiO_5[8]), which tend to exhibit higher strength at high temperatures. The sinterability of this formulation, however, is poor, and hot pressing or hot isostatic pressing is usually required to effect densification.[8–11] Also, because the β-Si_3N_4 network of elongated grains is less well-developed because of the more refractory liquid, the room-temperature toughness of these ceramics also is lower. The second approach focuses on the Si_3N_4–R_2O_3:9AlN binary. This composition forms a mixture of β-Si_3N_4 (or β-SiAlON) and α-SiAlON. The rare-earth cations mostly are stuffed in the interstices in the α-Si_3N_4 solid solution (e.g., α-SiAlON) and removed from grain boundaries; therefore, the ceramics of this composition have very little residual glassy phase and have achieved a strength of 1000 MPa at 1400°C.[12,13] The sinterability of these ceramics, however, also is poor, and hot pressing or gas-pressure sintering is required to form dense ceramics.[12–15] Also, there has been some recent concern of the dissolution of α-SiAlON over a long period of time at an intermediate temperature.[16–18] This, in turn, releases rare-earth cations and Al_2O_3 at the grain boundary and deteriorates properties.

We have reexamined the latter two sintering aid formulations, being aware of the phase relations, and have concluded that other more-promising formulations exist within the R_2O_3–

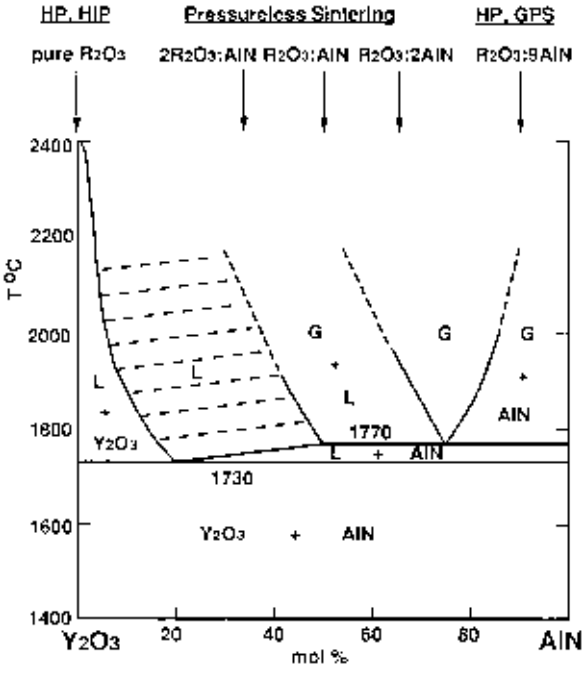

Fig. 1. Liquid region in Y_2O_3–AlN system.

S. C. Danforth—contributing editor

Manuscript No. 191770. Received June 3, 1996; approved November 27, 1996.
Supported by the U.S. Air Force Office for Scientific Research under Grant Nos. AFOSR-F49620-95-1 0119 and F-49620-95-1-0460.
Presented at the 98th Annual Meeting of the American Ceramic Society, Indianapolis, IN, April 14–17, 1996 (Basic Science Division, Paper No. B-34-96).
*Member, American Ceramic Society.

AlN family. Figure 1 shows the phase diagram of Y_2O_3–AlN to illustrate the point.[19] The two formulations described above correspond to either a region of a very high melting point, as in the case of pure R_2O_3, or a region where decomposition into a gaseous phase is favored, as in the case of R_2O_3:9AlN. However, there are many intermediate compositions in this system that form a liquid above 1730°C.[19] Very similar phase diagrams are valid for many other R_2O_3–AlN systems.[20] For example, Nd_2O_3–AlN has a eutectic temperature of 1660°C, and we expect the eutectic temperature to be somewhat lower when a combination of rare-earth oxides are used in conjunction with AlN. Because of the excellent high-temperature strength of Si_3N_4 ceramics sintered using either R_2O_3 or R_2O_3:9AlN additives, and the liquid-rich feature of the intermediate compositions between these two additives, we have decided to explore these intermediate compositions for pressureless sintering of Si_3N_4 in the present study.

II. Experimental Procedure

Compositions of 80 wt% Si_3N_4 and 20 wt% sintering aids, formulated on the Y_2O_3–La_2O_3–AlN ternary, were chosen for this study. In particular, we focused on the two compositions $2R_2O_3$:AlN and R_2O_3:AlN shown in Fig. 1, with R_2O_3 being a combination of Y_2O_3 and La_2O_3. The experimental procedure for starting materials and processing methods were similar to those described in our previous paper[21] and are briefly outlined below.

Powder mixtures were attrition milled in isopropyl alcohol for 2 h using Si_3N_4 milling media and teflon-coated containers. After they were milled, the powder mixtures were dried, sifted, isostatically pressed under 300 MPa, and then placed in a BN–Si_3N_4 mixed-powder-bed in a graphite crucible with a threaded cap. Pressureless sintering was conducted in a graphite furnace backfilled with 1 atm nitrogen gas at 1800°C for 3 h. Hot-pressing runs under 25 MPa at 1780°C for 1 h also were used to provide a reference to pressureless sintering. Some samples after sintering were further annealed at 1400°C for 15 h to crystallize the liquid phase.

Densified specimens were ground to remove 0.5 mm from the surfaces before density measurement and phase analysis. Density was measured by the Archimedean method using water, and the phase analysis was performed using X-ray diffraction (XRD). For lattice parameter determination, coarse silicon powders were used as an internal standard. Microstructural examination was performed in a scanning electron microscope (SEM) using polished specimens etched by plasma.

Bend bars with 1 mm × 3 mm × 20 mm dimensions were obtained from densified specimens. The surfaces of the specimens were finely ground along the long axis, then polished using a 6 μm diamond paste to obtain a good finish. For strength measurements, tests were conducted in nitrogen gas using a tungsten-mesh resistance furnace in a three-point bending configuration with a total span between outer supports at 13 mm. Vickers indentation at 10 kg was used to obtain hardness and to compute toughness from indentation cracking.[22]

III. Results and Discussion

(1) Sinterability and Additive Compositions

To verify that the intermediate compositions in the liquid-rich region are better sintering aids, the five formulations marked in Fig. 1 with different R_2O_3:AlN ratios have been investigated. Shown in Table I are sintered densities compared with hot-pressed densities, for the case where R_2O_3 is comprised of $(Y_{0.8}La_{0.2})_2O_3$ for the five formulations ranging from pure R_2O_3 to R_2O_3:9AlN. The three intermediate compositions of $2R_2O_3$:AlN, R_2O_3:AlN, and R_2O_3:2AlN have much superior sinterability.

We also have determined whether good sinterability can be achieved by varying the relative fraction of Y_2O_3 and La_2O_3 with no AlN. As shown in Table II, the sintered densities are always lower than the hot-pressed densities. However, the intermediate formulation of $(Y_{0.4}La_{0.6})_2O_3$ also is superior to other rare-earth oxide combinations.

The best combinations of oxides for the $2R_2O_3$:AlN and R_2O_3:AlN formulations are similarly determined from Table III. Highest relative densities are obtained at $(Y_{0.8}La_{0.2})_2O_3$ for both formulations, with the combination of $2(Y_{0.8}La_{0.2})_2O_3$:AlN especially outstanding because of its very low weight loss.

These density data are summarized graphically in Fig. 2 in terms of the composition of the three sintering additives, Y_2O_3, La_2O_3, and AlN. An extensive region, enclosed by a curved line, is delineated, within which the relative density exceeds 98%. This region has intermediate compositions of Y_2O_3, La_2O_3, and AlN. Also marked in Fig. 2 are the values of the total volume percent of the additive phases. The Y_2O_3–AlN side tends to have a higher volume fraction of additives at the same 20 wt%.

(2) Phase Assemblages

Phase assemblages have been analyzed and the results are summarized in Table IV. In all cases, β-Si_3N_4 is the dominant phase. We can detect very little difference between XRD reflections for this phase and those for the reference, pure Si_3N_4. If we assign the XRD peaks to $Si_{6-x}Al_xO_xN_{8-x}$ (β-SiAlON), our best estimate is that $x = 0.2$. The type of the dominant second phase, on the other hand, systematically varies with the additive composition. The systematic trend is best determined by inspection of the data of the annealed samples, which have more-developed phase assemblages. As the rare-earth oxide composition changes from Y_2O_3-rich to La_2O_3-rich, the dominant second phase changes from M′ melilite solid solution

Table I. Sinterability of Si_3N_4 (80 wt%) with Different $(Y_{0.8}La_{0.2})_2O_3$:AlN Ratios†

Property	$(Y_{0.8}La_{0.2})_2O_3$:AlN ratio				
	1:0	2:1	1:1	1:2	1:9
Sintered density (Mg/m^3)	3.294	3.477	3.443	3.407	3.160
Hot-pressed density (Mg/m^3)	3.467	3.475	3.450	3.417	3.317
Density ratio (%)	95.0	100	99.8	99.7	95.3

†Sintered at 1800°C for 3 h and hot pressed at 1780°C for 1 h.

Table II. Sinterability of Si_3N_4 with 20 wt% $(Y,La)_2O_3$ Additives†

Y:La molar ratio	Additive		Weight loss (wt%)	Density (Mg/m^3)		
	wt%	vol%		Hot pressed	Sintered	Ratio (%)
80:20	20	12.9	2.5	3.467	3.294	95.0
60:40	20	12.3	1.8	3.505	3.397	96.9
40:60	20	11.7	2.2	3.494	3.459	99.0
20:80	20	11.3	1.4	3.510	3.369	96.0

†Sintered at 1800°C for 3 h and hot pressed at 1780°C for 1 h.

Table III. Sinterability of Si_3N_4 with 20 wt% $2(Y,La)_2O_3$: AlN Additives and $(Y,La)_2O_3$:AlN Additives†

Y:La molar ratio	Additive wt%	Additive vol%	Weight loss (wt%)	Density (Mg/m^3) Hot pressed	Sintered	Ratio (%)
			$2(Y,La)_2O_3$:AlN			
100:0	20	14.2	2.1	3.459	3.294	95.2
90:10	20	13.8	2.9	3.468	3.392	97.8
80:20	20	13.5	0.3	3.475	3.477	100.0
60:40	20	12.9	1.1	3.483	3.461	99.4
40:60	20	12.3	2.1	3.488	3.449	98.9
20:80	20	11.8	3.0	3.508	3.401	96.9
0:100	20	11.4	5.5	3.531	3.279	92.9
			$(Y,La)_2O_3$:AlN			
80:20	20	14.0	1.3	3.450	3.443	99.8
60:40	20	13.4	1.3	3.455	3.438	99.5
40:60	20	12.8	2.0	3.489	3.454	99.0
20:80	20	12.3	3.7	3.494	3.214	92.0

†Sintered at 1800°C for 3 h and hot pressed at 1780°C for 1 h.

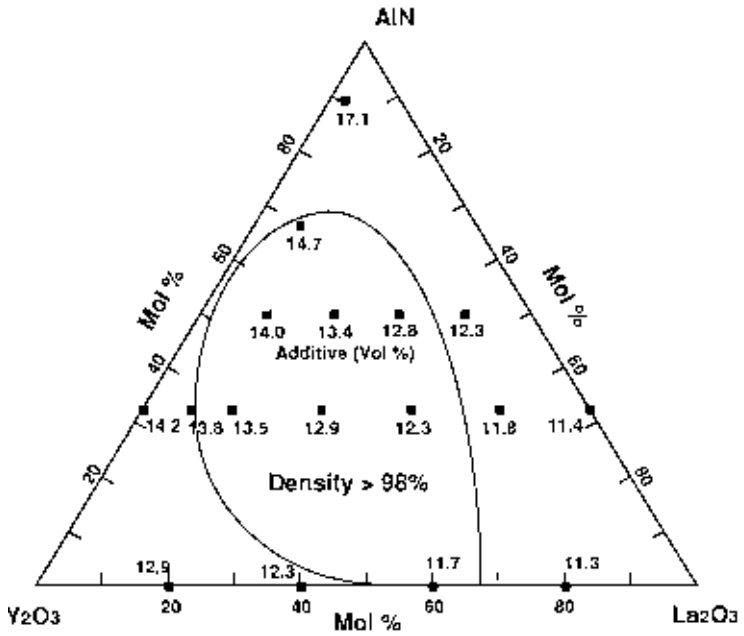

Fig. 2. Density map for Si_3N_4 in terms of sintering additives (20 wt%). Area where a relative density reaches no less than 98% is delineated. Numbers next to the filled squares are vol% of additives.

($R_2Si_{3-x}Al_xO_{3+x}N_{4-x}$), to K′ solid solution ($R_2Si_{2-x}Al_xO_{4+x}N_{2-x}$), to 1:2 phase ($La_2O_3{\cdot}2Si_3N_4$).

Lattice parameters of some of the dominant second phases have been determined to probe the extent of alloying in these solid solutions. These data also are listed in Table IV. In the absence of AlN, the melilite solid solution formed with $(Y_{0.8}La_{0.2})_2O_3$ additive has been identified as $(Y_{0.78}La_{0.22})_2Si_3N_4O_3$ using the interpolation formula reported by us[23] for rare-earth-containing melilite. Thus, the relative amount of yttrium and lanthanum in the solid solution is essentially similar to that of the overall formulation. In the absence of La_2O_3, the melilite solid solution formed with $2Y_2O_3$:AlN additive has been identified as $Y_2Si_{2.6}Al_{0.4}O_{3.4}N_{3.6}$, or $x = 0.4$, again using the interpolation formula. Thus, the extent of Al-O solution in this case is less than the maximum solubility that has been determined to be $x = 0.6$ for M′(Y).[23] This implies that the liquid formed in the present series of Si_3N_4 is not yet saturated with Al_2O_3. Assuming $x = 0.4$, we also have determined the composition of the melilite solid solution formed with $2(Y_{0.8}La_{0.2})_2O_3$:AlN to be $(Y_{0.85}La_{0.15})_2Si_{2.6}Al_{0.4}O_{3.4}N_{3.6}$. Thus, the Y:La ratio in this melilite probably also is similar to that of the overall composition. Lastly, comparing melilite solid solutions formed with $2(Y_{0.8}La_{0.2})_2O_3$:AlN and $(Y_{0.8}La_{0.2})_2O_3$:AlN additives, we find larger lattice parameters for the latter sintering conditions. The assumption that the rare-earth content is the same in both melilite solid solutions implies a higher x or Al-O content in the M′ formed with $(Y_{0.8}La_{0.2})_2O_3$:AlN additives. This is consistent with the higher amount of aluminum in the additives with a R_2O_3:AlN formulation than with a $2R_2O_3$:AlN formulation.

Overall, phase assemblages are only slightly changed by annealing, with the main difference being a more prominent presence of the second phases after annealing. An interesting observation has been made with the $2(Y_{0.6}La_{0.4})_2O_3$:AlN and $2(Y_{0.4}La_{0.6})_2O_3$:AlN additives: in both cases, XRD of the sintered ceramics contain only β-Si_3N_4 reflections and a broad hump from $2\theta = 28°$ to $2\theta = 33°$, indicating the presence of a substantial amount of glass but no crystalline second phase. The hump disappears after annealing; M′, K′, or 1:2 phase are found instead. Very similar observations also have been made for the other two sintering-aid formulations of R_2O_3:AlN and R_2O_3, where R is $Y_{0.6}La_{0.4}$ or $Y_{0.4}La_{0.6}$. Although the XRD of the sintered ceramics shows a broad hump from $2\theta = 28°$ to $2\theta = 33°$ and only β-Si_3N_4 reflections are seen, crystallization during annealing brings about M′ and K′ phases. Thus, the intermediate rare-earth oxide compositions apparently favor liquid formation and suppress crystallization. Lastly, it is a

Table IV. Phase Assemblages of Si_3N_4 (80 wt%) with Various Additives†

Y:La molar ratio	Phase assemblages‡ β	M′	K′	1:2	Lattice parameters, M (A)	Conditions
			$(Y,La)_2O_3$			
80:20	s	ms			7.647(4), 4.941(2)§	Sintered
60:40	s					Sintered
	s		s			Annealed
40:60	s					Sintered
	s		s			Annealed
20:80	s			m		Sintered
			$2(Y,La)_2O_3$:AlN			
100:0	s	ms			7.614(3), 4.922(2); $x = 0.4$¶	Sintered
	s	ms				Annealed
80:20	s	ms			7.643(3), 4.942(2); $x = 0.4$††	Sintered
	s	ms	m		7.666(6), 4.956(4)	Annealed
60:40	s					Sintered
	s	ms	m			Annealed
40:60	s					Sintered
	s		s	w		Annealed
20:80	s			mw		Sintered
	s			ms		Annealed
0:100	s			ms		Sintered
			$(Y,La)_2O_3$:AlN			
80:20	s	ms			7.655(4), 4.947(2)	Sintered
	s	s			7.662(6), 4.953(4)	Annealed
60:40	s					Sintered
	s	ms	w			Annealed
40:60	s					Sintered
	s	ms	w			Annealed
20:80	s			m		Sintered

†Sintered at 1800°C for 3 h and annealed at 1400°C for 15 h. ‡XRD intensity: s > ms > m > mw > w. §$(Y_{0.78}La_{0.22})_2Si_3O_3N_4$. ¶$^{Y}{}_2Si_{2.6}Al_{0.4}O_{3.4}N_{3.6}$, $x = 0.4$. ††$(Y_{0.85}La_{0.15})_2Si_{2.6}Al_{0.4}O_{3.4}N_{3.6}$, $x = 0.4$.

general observation that the lattice parameters of M′ solid solution increase slightly after annealing. This previously has been reported by us in a study of Si_3N_4/M′(R) and can be attributed to the further incorporation of Al-O into the solid solution.[21]

(3) Sinterability and Phase Relations

We already have emphasized, by referring to Fig. 1, the significance of liquid phase in the improved sinterability of Si_3N_4 with $2R_2O_3$:AlN and R_2O_3:AlN additives. By graphically summarizing the data in Table IV in the compositional triangle of Y_2O_3–La_2O_3–AlN, as shown in Fig. 3, we can compare it with Fig. 2 to further elucidate the pertinence of phase relations to sinterability of Si_3N_4. The compositions outside the high-density region delineated in Fig. 2 can be grouped into three types: pure oxides, 1:2 phase region, and gas-forming AlN-rich corner. According to Mitomo *et al.*,[24] La_2O_3–Si_3N_4 has a eutectic near 1600°C at about $3La_2O_3$:Si_3N_4. A similar liquid-forming region also has been found in Y_2O_3–Si_3N_4 binary at a higher temperature, 1720°C.[19] Thus, the relatively poor sinterability of Y_2O_3 additive is due to the higher melting temperature of the Y_2O_3–Si_3N_4 liquid. In the case of pure La_2O_3 and other lanthanum-rich additive compositions, we can similarly attribute their relatively poor sinterability to the high melting points of the 1:2 phase, which, according to Mitomo *et al.*,[24] is >2000°C. In contrast, M′(Y) solid solution has an intermediate melting point of ~1750°C, and probably a lower melting point for M′(Y,La) solid solution. Likewise, the intermediate compositions in Fig. 3 have a large liquid-forming region at 1800°C and, only after low-temperature annealing, form K′. Thus, under the sintering conditions used in the present study, 1800°C with 1 atm nitrogen gas, we expect copious liquid to form and to maintain for all the additives that have compositions within the high-density region shown in Fig. 2.

Although the above discussion mostly is based on the R_2O_3–AlN binary, consideration of the R_2O_3–AlN–Si_3N_4 ternary and surface oxides is not expected to fundamentally alter the basic picture. A recent study of solid–liquid reaction in the Si_3N_4–AlN–Y_2O_3 system under 1 MPa of nitrogen gas has established a ternary eutectic temperature of 1650°C,[19] which is ~80°C lower than the eutectic temperature of the Y_2O_3–AlN binary. Because surface oxides also are involved in the powders of the latter study, the above temperature is representative of our experimental conditions as well. The eutectic temperature of SiO_2–Al_2O_3–Y_2O_3 is much lower. However, the amount of the liquid phase formed is too small to cause sufficient sintering, as we previously have demonstrated in a series of kinetic studies.[25,26] Thus, it seems certain that it is the high-temperature eutectics in R_2O_3–AlN and in R_2O_3–AlN–Si_3N_4, which bear the same feature, that are most pertinent to sinterability of these ceramics.

Analysis of compatibility relations manifest in the phase assemblages listed in Table IV further allows us to construct Fig. 4, which outlines major phases in the La-Y-Si-O-N system.[27] Three phases—M′(Y,La) and K′(Y,La) solid solutions, as well as 1:2—are compatible with β-Si_3N_4. The pyramid formed by joining the Si_3N_4 apex and the M′(Y,La)/K′(Y,La) base is especially noteworthy in that all compositions therein appear readily sinterable with a small addition of AlN. In the present study, the amount of AlN ranges from 1.3 to 5.0 wt% (some substitution of Al-O for Si-N throughout the pyramid is likely in the presence of AlN sintering aid). As shown below, the mechanical properties of these Si_3N_4 ceramics are generally quite promising.

(4) Microstructure and Mechanical Properties

Experiments on the mechanical properties were conducted to assess their merits as structural materials. Test specimens were selected from three composition groups investigated and included essentially all the high-density ceramics. The test results on sintered ceramics are summarized in Table V, including strength (at room temperature and 1200°C), hardness, and toughness (at room temperature). For sintered samples that had a strength at 1200°C <600 MPa, annealing also was conducted, and the 1200°C strength subsequently was measured again.

The results are briefly discussed below.

(A) Hardness: Hardness values are typical of Si_3N_4 ceramics, and they increase with a higher AlN:R_2O_3 ratio and a higher Y_2O_3:La_2O_3 ratio. This is reasonable because the bond strength of the three additives follows the sequence of AlN >

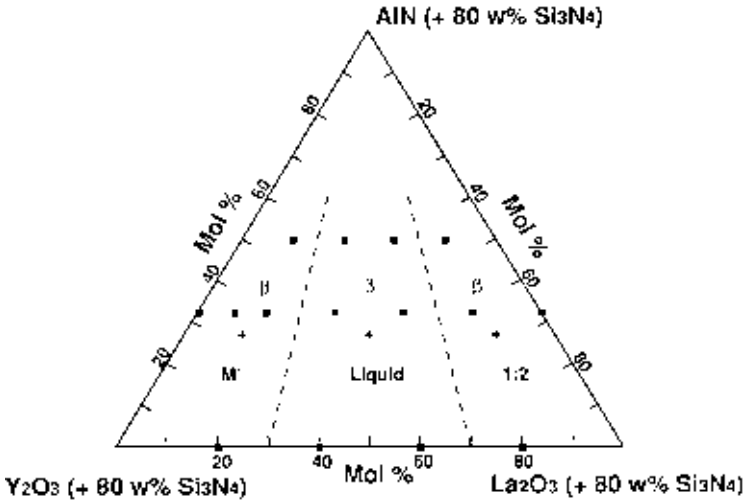

Fig. 3. Phase assemblages in the system $(Y,La)_2O_3$–AlN–Si_3N_4 after sintering at 1800°C for 3 h.

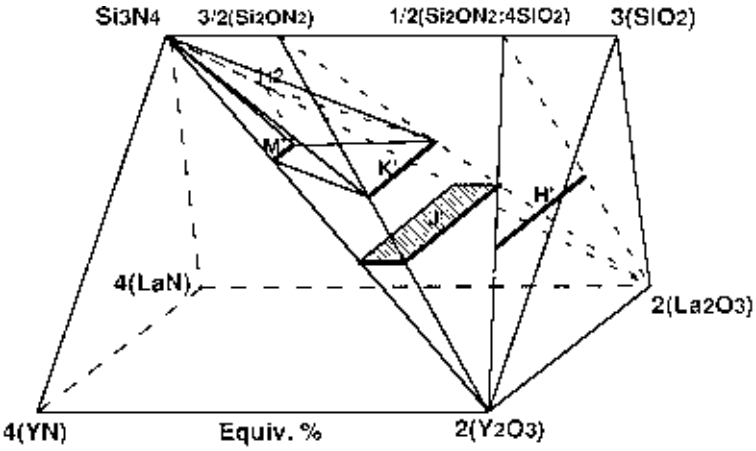

Fig. 4. Phases in La-Y-Si-O-N system: (a) 1:2, $La_2Si_6O_3N_8$; (b) M′, $(Y,La)_2Si_3O_3N_4$; (c) K′, $(Y,La)_2Si_2O_4N_2$; (d) J′, $(Y,La)_4Si_2O_7N_2$; and (e) H′, $(Y,La)_5Si_3O_{12}N$.

Table V. Mechanical Properties for Selected Specimens of Si_3N_4 wih Various Additives†

Y:La ratio	Bend strength (MPa) Room temperature	1200°C Sintered	1200°C Annealed	Hardness, H_v (GPa)	Toughness, K_{Ic} (MPa·m$^{1/2}$)
		$(Y,La)_2O_3$			
60:40	800	380	630	14.3	7.7
40:60	780	410	490	14.2	7.5
		$2(Y,La)_2O_3$:AlN			
80:20	890	1150		15.3	6.8
60:40	910	590	590	15.2	5.6
40:60	790	530	615	14.5	6.0
20:80	610	740		12.4	7.0
		$(Y,La)_2O_3$:AlN			
80:20	950	650		16.4	7.8
40:60	710	560	460	15.4	6.2

†Sintered at 1800°C for 3 h and annealed at 1400°C for 15 h.

$Y_2O_3 > La_2O_3$. The relatively low hardness of $2(Y_{0.2}La_{0.8})_2O_3$:AlN is probably due to a lower density (97%) for the specimen.

(B) Toughness: Typical toughness is ~7.0 MPa·m$^{1/2}$. Microstructural examination of ceramics sintered with all three groups of additives shows a network of elongated, rod-shaped grains of β-Si_3N_4. Typical micrographs are shown in Fig. 5 for a Si_3N_4 sintered with $2(Y_{0.8}La_{0.2})_2O_3$:AlN sintering aids. Such a microstructure is known to impart high toughness via grain bridging and pullout in the crack wake.[28,29] This microstructure also is similar to those of other high-toughness Si_3N_4 reported in the literature.

(C) Strength at Room Temperature and 1200°C: Strength at room temperature mostly is flaw controlled and should correlate with the sintered density. For the three ceramics that had the highest strengths, 950 MPa with $(Y_{0.8}La_{0.2})_2O_3$:AlN sintering aid, 890 MPa with $2(Y_{0.8}La_{0.2})_2O_3$:AlN sintering aid, and 910 MPa with $2(Y_{0.6}La_{0.4})_2O_3$:AlN sintering aid, the densities are all >99%. Strength at high temperature is mostly governed

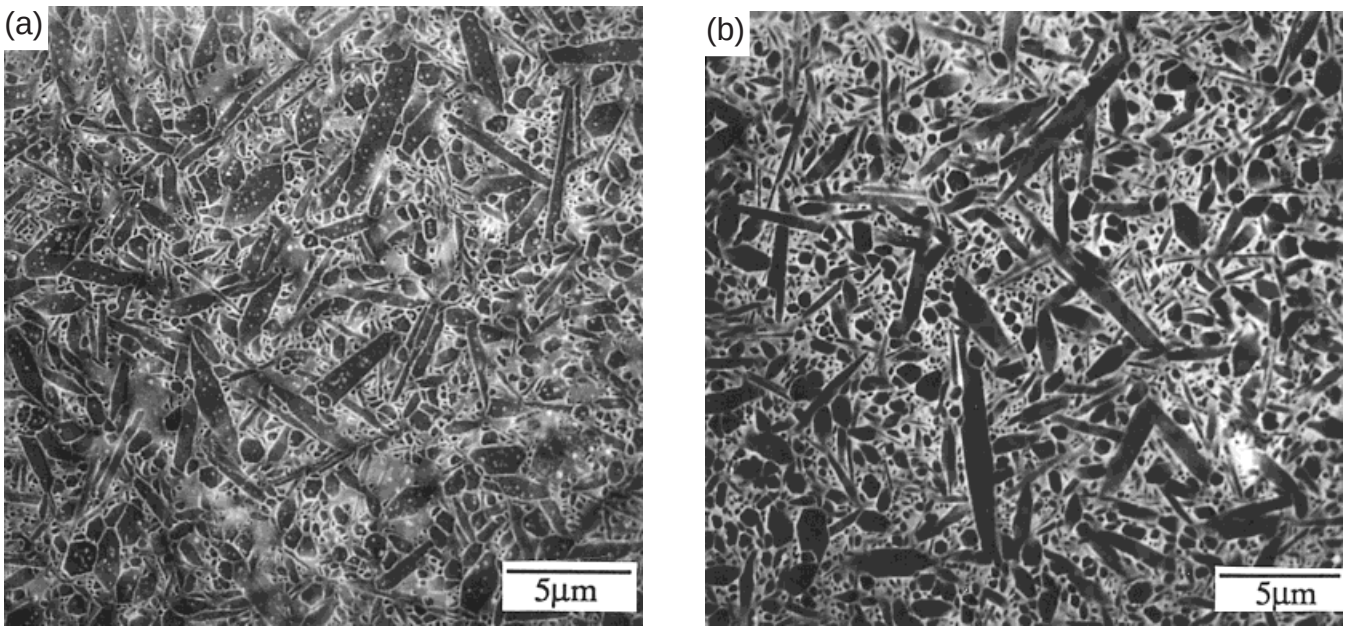

Fig. 5. SEM micrographs for Si_3N_4 with $2(Y_{0.8}La_{0.2})_2O_3$:AlN additives: (a) as sintered and (b) after annealing.

by the softening temperature of the grain-boundary phase. In this series of ceramics, a strength of 1150 MPa at 1200°C has been achieved using $2(Y_{0.8}La_{0.2})_2O_3$:AlN as additive. For those ceramics that have a relatively low strength (<600 MPa) at 1200°C, annealing proves effective in improving the strength. This is especially so with intermediate Y_2O_3:La_2O_3 compositions, which, as noted previously, tend to retain the liquid phase after sintering.

The temperature dependence of strength was investigated using the ceramic sintered with $2(Y_{0.8}La_{0.2})_2O_3$:AlN aid. Figure 6 shows that strength decreases initially with temperature before increasing to a maximum at 1200°C, followed by a steep fall at 1400°C. Such behavior has been reported in the past for both Si_3N_4[30,31] and other ceramics[32–34] that contain elongated grains and a significant amount of glassy grain-boundary phases. The peak strength temperature is rationalized to correspond to the onset of the glass softening upon which pullout of grains becomes commonplace while the frictional work remains substantial.[28,29]

IV. Conclusions

Pressureless sintering of fully dense Si_3N_4 ceramics, of high strength at high temperature and high toughness at room temperature, is possible using liquid-rich Y_2O_3–La_2O_3–AlN additives of an intermediate composition. The overall compositions are located in the Si_3N_4–M′(Y,La)/K′(Y,La) pyramid in the Janecke prism of the La-Y-Si–O-N system, with only some small addition of AlN. The terminal Y_2O_3, La_2O_3, and AlN-rich compositons are not desirable sintering aids because of high liquidus temperature (Y_2O_3–Si_3N_4), compound formation ($La_2O_3 \cdot 2Si_3N_4$), and gas formation, respectively.

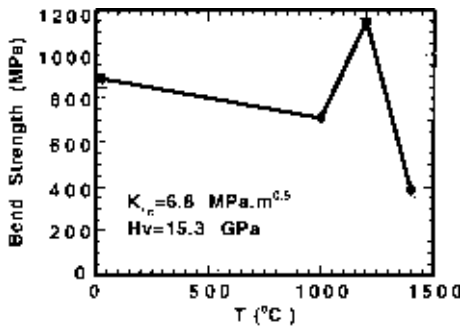

Fig. 6. Strength of Si_3N_4 with $2(Y_{0.8}La_{0.2})_2O_3$:AlN additive.

Sintered ceramics contain essentially β-Si_3N_4 and a glass that crystallizes into M′(Y,La) or K′(Y,La) solid solutions. A network of elongated, rod-shaped Si_3N_4 grain forms, resulting in high toughness at room temperature. The softening points of the grain-boundary phases probably lie around 1200°C. Strengths of 900 MPa at room temperature and 600–1150 MPa at 1200°C have been achieved in these ceramics.

References

[1]A. Tsuge, K. Nishida, and M. Komatsu, "Effect of Crystallizing the Grain-Boundary Glass Phase on the High-Temperature Strength of Hot-Pressed Si_3N_4 Containing Y_2O_3," *J. Am. Ceram. Soc.*, **58**, 323–26 (1975).

[2]K. Komeya, "Development of Nitrogen Ceramics," *Am. Ceram. Soc. Bull.*, **63** [9] 1158–64 (1984).

[3]E. Tani, S. Umebayashi, K. Kishi, K. Kobayashi, and M. Nishijima, "Gas-Pressure Sintering of Si_3N_4 with Concurrent Addition of Al_2O_3 and 5 wt% Rare-Earth Oxide: High Fracture Toughness Si_3N_4 with Fiber-Like Structure," *Am. Ceram. Soc. Bull.*, **65** [9] 1311–15 (1986).

[4]S. Boskovic, L. J. Gauckler, G. Petzow, and T. Y. Tien, "Reaction Sintering Forming β-Si_3N_4 Solid Solutions in the System Si,Al/N,O. I: Sintering of SiO_2–AlN Mixtures; II: Sintering of Si_3N_4–SiO_2–AlN Mixtures; and III. Sintering of Si_3N_4–AlN–Al_2O_3 Mixtures," *Powder Metall. Int.*, **9** [4] 185 (1977); *ibid.*, **10** [4] 184 (1978); and *ibid.*, **11** [4] 169 (1979).

[5]K. Komeya, M. Komatsu, T. Kameda, Y. Goto, and A. Tsuge, "High-Strength Silicon Nitride Ceramics Obtained by Grain Boundary Crystallization," *J. Mater. Sci.*, **26**, 5513–16 (1991).

[6]A. Rendtel, H. Hubner, and C. Schubert, "Improvements in the Creep Strength of HPSN by Optimization of Additive Content and Thermal Treatment"; pp. 593–98 in *Proceedings of the International Conference on Silicon Nitride-Based Ceramics, Key Engineering Materials*, Vol. 89–91 (Stuttgart, Germany, Oct. 4–6, 1993). Edited by M. J. Hoffmann, P. F. Becher, and G. Petzow. TransTech Publications, Aedermannsdorf, Switzerland, 1994.

[7](a) C. O'Meara, G. L. Dunlop, and R. Pompe, "Phase Relationships in the System SiO_2–Y_2O_3–Al_2O_3," *Mater. Sci. Monogr.*, **38A** [High Tech. Ceram., Pt. A] 265–70 (1987). (b) R. S. Roth; Fig. 9646 in *Phase Diagrams for Ceramists*. Edited by M. A. Clevinger. American Ceramic Society, Westerville, OH, 1995.

[8]M.. Herrmann, H. Klemm, C. Schubert, K. Tangermann, T. Reich, and H. Kruner, "High-Temperature Properties of Silicon Nitride Materials with Rare-Earth Additives"; pp. 211–14 in *Proceedings of 5th International Symposium on Ceramic Materials and Components for Engines* (May 29–June 1, 1994, Shanghai, China). Edited by D. S. Yan, X. R. Fu, and S. X. Shi. World Scientific, Singapore. 1994.

[9]Y. R. Xu, T. S. Yen (D. S. Yan), and X. R. Fu, "Grain-Boundary Tailoring of High-Performance Nitride Ceramics and Their Creep Property Studies"; pp. 739–50 in *Proceedings of the 3rd International Symposium on Ceramic Materials and Components for Engines*. American Ceramic Society, Westerville, OH, 1989.

[10]T. S. Yen, "High-Performance Silicon Nitride Composite Ceramics through Grain-Boundary and Microstructural Tailoring"; pp. 137–48 in *Tailoring*

of Mechanical Properties of Si_3N_4 Ceramics, Vol. 276, NATO ASI Series, Series E: Applied Sciences. Edited by M. J. Hoffmann and G. Petzow. Kluwer, Dordrecht, The Netherlands, 1993.

[11]P. O. Olsson and T. Ekstrom, "HIP-Sintered β- and Mixed α-β-SiAlONs Densified with Y_2O_3 and La_2O_3 Additions," *J. Mater. Sci.*, **25**, 1824–32 (1990).

[12]Y. Ukyo and S. Wada, "High-Strength Si_3N_4 Ceramics," *Nippon Seramikkusu Kyokai Gakujutsu Ronbunshi*, **97** [8] 872–74 (1989).

[13]S. Wada and Y. Ukyo, "Microstructure and Properties of α/β-SiAlON Composite"; pp. 29–33 in *Proceedings of 34th Japan Congress on Materials Research*. Society of Materials Science, Kyoto, Japan, 1991.

[14](a) L. J. Dong, Z. K. Huang, W. Y. Sun, and L. P. Huang, "β:α-SiAlON Composites by GPS"; Presented at the 93rd Annual Meeting of American Ceramic Society, Cincinnati, OH, May 1, 1991 (Ceramic Matrix Composite Symposium, Paper No. 106-SVI-91). (b) "The Fabrication of β:α-SiAlON Composite Ceramics (in Chin.), *Spark Plug and Special Ceramics*, **1**, 18–22 (1993).

[15]T. S. Sheu, "Microstructure and Mechanical Properties of the *in situ* β-Si_3N_4/α-SiAlON Composite," *J. Am. Ceram. Soc.*, **77** [9] 2345–53 (1994).

[16]Y. Ukyo, N. Sugiyama, and S. Wada, "Thermal Stability of Y-α-SiAlON Co-existing with β-SiAlON"; pp. 141–46 in *Proceedings of 1st International Symposium on the Science of Engineering Ceramics* (Oct. 21–23, 1991, Koda, Japan). Edited by S. Kimura and K. Niihara. Ceramic Society of Japan, Tokyo, Japan, 1991.

[17]H. Mandal, D. P. Thompson, and T. Ekstrom, "Reversible α–β-SiAlON Transformation in Heat-Treated Sialon Ceramics," *J. Eur. Ceram. Soc.*, **12**, 421–29 (1993).

[18]Z. J. Shen, T. Ekstrom, and M. Nygren, "Temperature Stability of Samarium-Doped α-SiAlON Ceramics," *J. Eur. Ceram. Soc.*, **16** [1] 43–53 (1996).

[19]Z. K. Huang and T. Y. Tien, "Solid–Liquid Reaction in the Si_3N_4–AlN–Y_2O_3 System," *J. Am. Ceram. Soc.*, **79** [6] 1717–19 (1996).

[20]Z. K. Huang, D. S. Yan (T. S. Yen), and T. Y. Tien, "Compound Formation and Melting Behavior in the AB Compound and Rare-Earth Oxide Systems," *J. Solid State Chem.*, **85**, 51–55 (1990).

[21]Z. K. Huang, S. Y. Liu, A. Rosenflanz, and I-W. Chen, "SiAlON Composites Containing Rare-Earth Melilite and Neighboring Phases," *J. Am. Ceram. Soc.*, **79** [8] 2081–90 (1996).

[22]G. R. Anstis, P. Chantikul, B. R. Lawn, and D. B. Marshall, "A Critical Evaluation of Indentation Techniques for Measuring Fracture Toughness: I. Direct Crack Measurements," *J. Am. Ceram. Soc.*, **64** [9] 533–38 (1981).

[23]Z. K. Huang and I-W. Chen, "Rare-Earth Melilite Solid Solution and Its Phase Relations with Neighboring Phases," *J. Am. Ceram. Soc.*, **79** [8] 2091–97 (1996).

[24]M. Mitomo, F. Izumi, S. Horiuchi, and Y. Matsui, "Phase Relationships in the System Si_3N_4–SiO_2–La_2O_3," *J. Mater. Sci.*, **17**, 2359–64 (1982).

[25]M. Menon and I-W. Chen, "Reaction Densification of α-SiAlON: I, Wetting Behavior and Acid–Base Reactions," *J. Am. Ceram. Soc.*, **78** [3] 545–52 (1995).

[26]M. Menon and I-W. Chen, "Reaction Densification of α-SiAlON: II, Densification Behavior," *J. Am. Ceram. Soc.*, **78** [3] 553–59 (1995).

[27]G. Z. Cao, Z. K. Huang, and D. S. Yan, "Phase Relationships in the Si_3N_4–Y_2O_3–La_2O_3 System," *Sci. Sin., Ser. A*, **11**, 1212–16 (1988).

[28]I-W. Chen, S. Y. Liu, and D. Jacobs, "Effects of Temperature, Rate, and Cyclic Loading on the Strength and Toughness of Monolithic Ceramics," *Acta Metall. Mater.*, **43** [4] 1439–46 (1995).

[29]P. F. Becher, H. T. Lin, S. L. Hwang, M. J. Hoffmann, and I-W. Chen, "The Influence of Microstructure on the Mechanical Behavior of Silicon Nitride Ceramics"; pp. 147–58 in Materials Research Society Symposium Proceedings, *Silicon Nitride Ceramics, Science, and Technical Advances*, Vol. 287 (Boston, MA, Nov. 30–Dec. 3, 1992). Edited by I-W. Chen, P. F. Becher, M. Mitomo, G. Petzow, and T. S. Yen. Materials Research Society, Pittsburgh, PA, 1993.

[30]S. H. Knickerbocker, A. Zangvil, and S. D. Brown, "Displacement-Rate and Temperature Effect in Fracture of Hot-Pressed Silicon Nitride at 1100° to 1325°C," *J. Am. Ceram. Soc.*, **67** [5] 365–68 (1984).

[31]Y. Mutoh, K. Yamaishi, N. Miyahara, and T. Oikawa, "Brittle to Ductile Transition in Silicon Nitride"; pp. 427–40 in *Fracture Mechanics of Ceramics*, Vol. 10. Edited by R. C. Bradt *et al.* Plenum Press, New York, 1992.

[32]A. G. Crough and K. H. Jolliffe, "The Effect of Stress Rate on the Rupture Strength of Alumina and Mullite Refractories," *Proc. Br. Ceram. Soc.*, **15**, 37–46 (1970).

[33]R. W. Davidge and G. Tappin, "The Effect of Temperature and Environment on the Strength of Two Polycrystalline Aluminas," *Proc. Br. Ceram. Soc.*, **15**, 47–60 (1970).

[34]B. J. Dalgleish, A. Fakhr, P. L. Pratt, and R. D. Rawlings, "The Temperature Dependence of the Fracture Toughness and Acoustic Emission of Polycrystalline Alumina," *J. Mater. Sci.*, **14**, 2605–15 (1979). □